BUTTERWORTH HEINEMANN

Polymer Vol. 36, No. 14, pp. 2753–2760, 1995

0032-3861/95/$10.00+0.00

Microphase vs. macrophase formation in homopolymer/block copolymer blends with exothermic interaction

Adeyinka Adedeji, Alex M. Jamieson* and Steven D. Hudson
Department of Macromolecular Science, Case Western Reserve University, Cleveland, OH 44106, USA
(Received 6 December 1994)

The formation of a microphase and a macrophase in solvent-cast homopolymer/block copolymer blends, where the homopolymer is exothermically miscible with one of the block copolymer segments, is demonstrated to depend on the molecular weights of the homopolymer and the incompatible segment of the block copolymer, in spite of the exothermic mixing. Binary blends of poly(vinyl chloride) (PVC) with poly(n-butyl methacrylate-*b*-styrene) (PnBMA-*b*-PS) block copolymer, solvent cast from methyl ethyl ketone, were investigated. By varying the molecular weight, we vary the thermodynamic product $N\chi_{PVC/PS}$ which controls the phase morphology. Here $N = N_{PVC}N_{PS}/(N_{PVC}^{1/2} + N_{PS}^{1/2})^2$, where N_{PVC} and N_{PS} are the degrees of polymerization of PVC and PS block copolymer segment, respectively, and $\chi_{PVC/PS}$ is the Flory–Huggins parameter which characterizes the repulsive interaction between PVC and PS. Microphase separation is observed when $N\chi_{PVC/PS}$ is small; and when $N\chi_{PVC/PS}$ is large, macrophase or macrophase-induced microphase separation occurs. The routes of phase formation are discussed using equilateral triangular phase diagrams, and a morphology diagram is constructed for homopolymer/block copolymer blends. Microphase formation is observed even when the molecular weight of the homopolymer is much larger than that of the miscible block copolymer segment, and when the homopolymer is polydisperse. Indeed, since macrophase formation occurs when N is large, it is clear that low molecular weight block copolymer is necessary to form the microphase when a homopolymer of high molecular weight is present.

(Keywords: microphase; macrophase; blends)

INTRODUCTION

There is an abundant literature on the compatibilization of blends of homopolymers with block copolymers both when the chemistries of the homopolymer and one of the block copolymer segments are similar[1–10] (i.e. in A/A-*b*-B blends) and when the homopolymers exothermically mix with the block copolymer segments[11–21] (i.e. in A/X-*b*-B, where all the components have different chemistries). In particular, when a homopolymer mixes exothermically with one segment of a block copolymer it has been shown experimentally[13–16,18–21] and theoretically[11–13,15,17,18,20] that the favourable enthalpic interaction is a strong driving force towards microphase separation. An important observation[20] in this case is that a high molecular weight homopolymer effectively wets a block copolymer brush whose molecular weight is much smaller (i.e. when $M_h/M_x \gg 1$). This interfacial solubilization arises because the free energy is lowered by maximizing the homopolymer segmental contact with the compatible block copolymer segment. Thus in the presence of exothermic interaction, emulsification of polydisperse homopolymers is facilitated[13,20]. These results suggest that exothermic interactions will also be an effective aid in compatibilizing immiscible polymer blends with a block copolymer. It should, however, be realized that the repulsions between the dissimilar segments of the block copolymer and between the homopolymer and the incompatible block segment are each an additional driving force for microphase formation in homopolymer/block copolymer blends[15,22], and for interfacial activity when a block copolymer is used as a compatibilizer in immiscible blends[23]. A simple schematic illustration is presented in *Figure 1* to denote the different pair interactions in an A/X-*b*-B homopolymer/block copolymer blend with exothermic interaction between A and X. Note that the repulsion between copolymer segments X and B generates microphase segregation in pure X-*b*-B block copolymer; the A/B[24,25] and X/B repulsions are each a driving force for microphase segregation in A/X-*b*-B blends. However, the A/B repulsion can lead to macrophase segregation of X-*b*-B from homopolymer A, despite a favourable exothermic mixing of the homopolymer A with segment X, if the A/B repulsion is very strong.

The influence that the A/B repulsive interaction can have on the segregation behaviour of the block copolymer has not received enough attention both experimentally and theoretically. Note that the repulsion between the block copolymer segments X and B ($\chi_{X/B}$) can lead only to microphase separation, and no matter how large the magnitude of the product

* To whom correspondence should be addressed

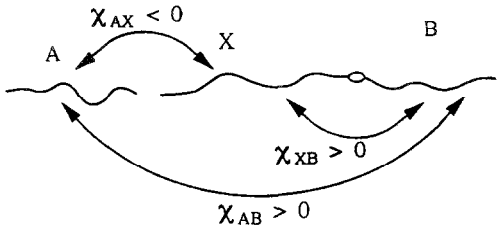

Figure 1 Schematic illustration of the enthalpic repulsions (i.e. positive $\chi_{X/B}$ and $\chi_{A/B}$) in a binary homopolymer/block copolymer blend. Note that $\chi_{A/X}$ is exothermic

$N_{X/B}\chi_{X/B}$, where $N_{X/B}$ is the block copolymer molecular weight, it cannot induce macrophase separation. Hence, macrophase separation is attributable only to the repulsion between homopolymer A and the incompatible segment B. Hashimoto *et al.*[21] have investigated concentration fluctuations in blends of poly(phenylene oxide) (PPO) homopolymers with poly(styrene-*b*-isoprene) block copolymers using transmission electron microscopy (TEM). The spatial extent of PPO concentration fluctuations was indicated by a modulation of the microstructure on a length scale typical of macrophase separation. Such a structural development was explained as resulting from an initial macrophase separation, leading to regions respectively rich and poor in block copolymer, which is followed by microphase separation to generate the different microstructures. This mechanism has been termed macrophase-induced microphase separation, since the geometries of the microstructures are dictated by the local concentration of the block copolymer which results from the prior macrophase transition[26]. The definition of microphase separation, in this context, is a segregation of a homogeneous phase over a length scale of the molecular chain dimension (~10 nm), and the macrophase transition is a structural modulation that exists over a length scale comparable to 1 μm. A convenient representation of the processes of microphase and macrophase formation via the ternary homopolymer/block copolymer/solvent phase diagram was presented[21]. The final morphology was attributed to the strong long range repulsion between PPO and the polyisoprene (PI) block segment.

In addition, Lowenhaupt *et al.*[15] have evaluated the structure factor of the incompatible component B in a binary A/X-*b*-B mixture within the random phase approximation (RPA). A comprehensive analysis was carried out of the critical values of block copolymer composition, relative chain length of A and segment X, favourable Flory–Huggins parameter $\chi_{A/X} < 0$, and temperature at which the microphase will transform to macrophase. It was found that only a very small favourable enthalpic interaction is needed to generate mixing between the homopolymer A and the block segment X, even when the molecular weight of the homopolymer (M_h) is much larger than that of the block segment (M_x), and that the critical volume fraction f of the block copolymer at which the microphase transforms to macrophase increases with increasing ratio λ, where $\lambda = M_h/M_x$. An observation of particular interest was made by these authors in the experimental section, where it is reported that macrophase separation is obtained at most compositions in blends of polycarbonate (PC) with poly(methyl methacrylate-*b*-styrene) (PMMA-*b*-PS), even though PC is marginally miscible with PMMA homopolymer. However, the RPA model predicts only microphase separation in such a blend combination over all compositions. The discrepancy appears to arise because the repulsion between PC and PS ($\chi_{A/B} = \chi_{PC/PS} > 0$) was ignored in their RPA model. Moreover, the case where $\chi_{A/X} < 0$ and $\lambda < 1$ was not discussed.

In this study, we investigate the effect of a strong repulsion between the homopolymer A and the block segment B on the process of phase formation in A/X-*b*-B blends. The magnitude of the repulsion is characterized by the product $N\chi_{A/B}$ as recommended by Leibler[27], and we arrange that the block copolymer remains nearly symmetrical, i.e. $f \approx 0.5$. The product $N\chi_{A/B}$ can be varied by changing either N or $\chi_{A/B}$. Note that N is an effective molecular weight of the mutually repulsive polymer pair, $N = N_{PVC}N_{PS}/(N_{PVC}^{1/2} + N_{PS}^{1/2})^2$, and that N can be changed by varying the molecular weight of either of the polymers. Binary blends of poly(vinyl chloride) (PVC) with poly(n-butyl methacrylate-*b*-styrene) (PnBMA-*b*-PS) were chosen for this study. Here $\chi_{A/B}$ is $\chi_{PVC/PS}$ since PVC repels the PS block segment. The relative tendency for microphase vs. macrophase formation can be manipulated by changing the molecular weight of the PVC and that of the block copolymer, which alters $N\chi_{PVC/PS}$. PVC homopolymer is known to be miscible with PnBMA[22–25,27–30] because of weak intermolecular hydrogen bonding[31], and $\chi_{PVC/PnBMA} = -0.92$ has been reported by Walsh and McKeown[28]. Hence, a binary PVC/PnBMA-*b*-PS blend is an example of the A/X-*b*-B system described earlier. In the analysis of this blend, the repulsion between the PnBMA and PS segments of the PnBMA-*b*-PS block copolymer is assumed to contribute only to microphase formation.

EXPERIMENTAL

The characteristics and acronyms of the polymer species used in this study are presented in *Table 1*. Solutions of PVC and block copolymers were made in methyl ethyl ketone (MEK) at a concentration of 1 g per 100 ml. One set of binary blends was made by mixing 20 vol% of B(130) or B(440) with 80 vol% of PVC(78), PVC(120), PVC(175), PVC(275) or PVC(500). The second set of blends was made by mixing 80 vol% of B(440) with 20 vol% of PVC(78), PVC(120), PVC(175), PVC(275) or PVC(500). The solvent was slowly evaporated over seven days at room temperature, and the final traces of the

Table 1 Characteristics of the homopolymers and the block copolymers

Polymer	$10^{-3}M_w$ (Da)	Abbreviation	Inherent viscosity	M_w/M_n
PVC[a]	78	PVC(78)	0.65	2.00
PVC[b]	120	PVC(120)	0.65	
PVC[b]	175	PVC(175)	0.90	
PVC[b]	275	PVC(275)	1.38	
PVC[a]	500	PVC(500)	1.40	5.32
PnBMA-*b*-PS[c]	76/54	B(130)		1.06
PnBMA-*b*-PS[c]	225/215	B(440)		1.14

[a] Purchased from Sigma
[b] Purchased from Scientific Polymer Products
[c] Purchased from Polysciences

solvent were removed by drying at 70°C for 24 h at atmospheric pressure, then under vacuum for another 24 h.

The solvent-free films (~0.4 mm thick) were sectioned, using a Microstar diamond knife, with an RMC MT-7000 ultramicrotome machine in a direction normal to the surface to obtain thin films (70–90 nm thick) which were subsequently exposed to RuO_4 vapour for 45 min in an enclosed chamber containing 1.5% aqueous solution of RuO_4. The PS segment of the PnBMA-*b*-PS block copolymer in the specimen was stained with the RuO_4. Bright field images were obtained by mass/thickness contrast on a JEOL JEM-100SX transmission electron microscope at 100 kV. The PS minor phase appeared as the darkest regions in the TEM micrographs.

RESULTS AND DISCUSSION

Electron micrographs of blends containing 80 vol% PVC with 20 vol% B(130) are shown in *Figures 2a–e* in

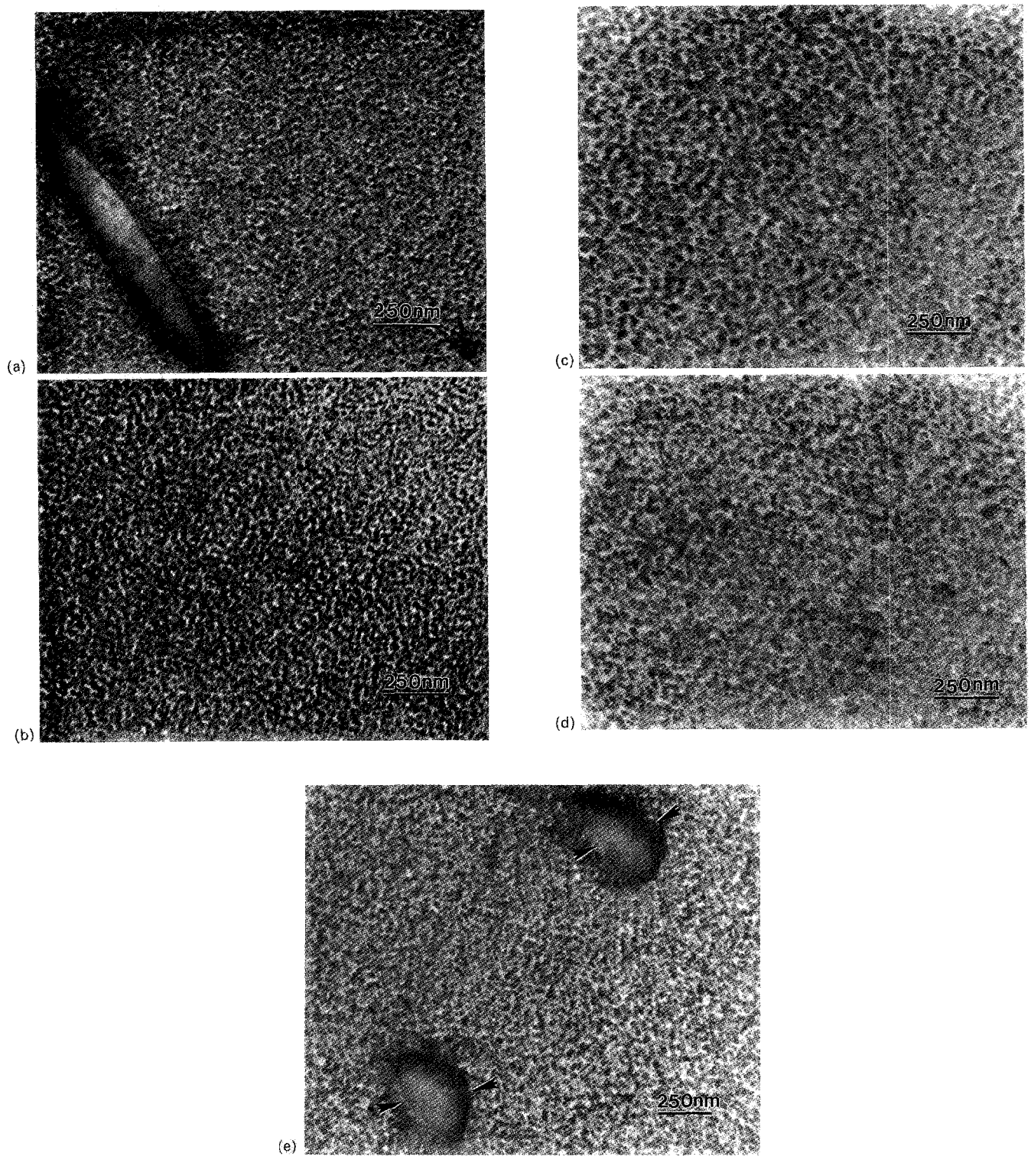

Figure 2 The microphase and macrophase formed in binary PVC/PnBMA-*b*-PS blends containing 20 vol% B(130): (a) PVC(78)/B(130); (b) PVC(120)/B(130); (c) PVC(175)/B(130); (d) PVC(275)/B(130); (e) PVC(500)/B(130)

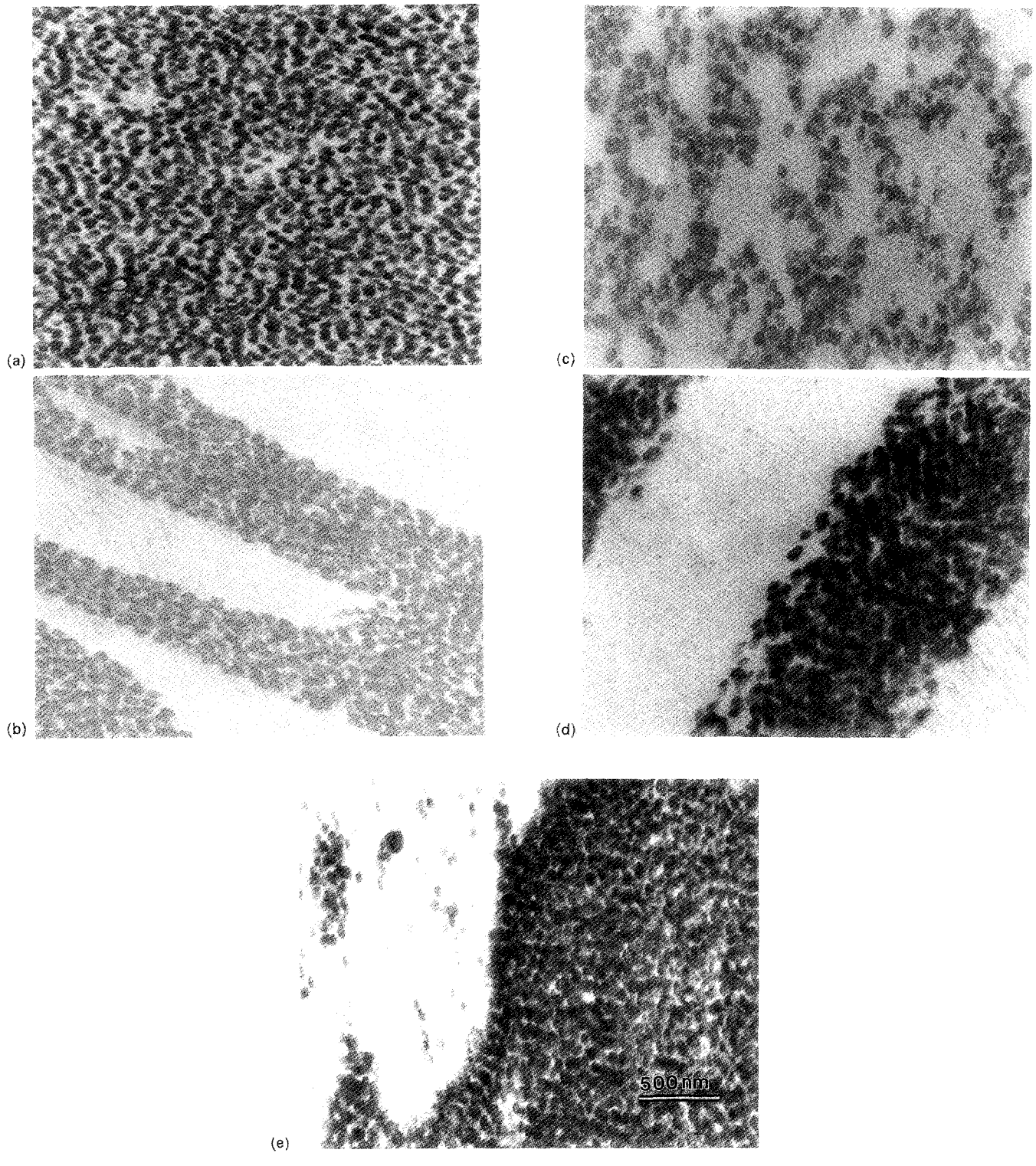

Figure 3 The microphase and macrophase formed in binary PVC/PnBMA-*b*-PS blends containing 20 vol% B(440): (a) PVC(78)/B(440); (b) PVC(120)/B(440); (c) PVC(175)/B(440); (d) PVC(275)/B(440); (e) PVC(500)/B(440)

increasing order of PVC molecular weight. Those of blends containing 80 vol% PVC with 20 vol% B(440) are displayed in *Figures 3a–e* in increasing order of PVC molecular weight. Micrographs of blends containing 80 vol% B(440) with 20 vol% PVC(120), PVC(175) or PVC(275) are presented in *Figures 4a–c*, respectively. Ratios of the molecular weights of the homopolymer PVCs to those of the compatible PnBMA block segments (M_h/M_x) and the corresponding magnitudes of the product $N\chi_{PVC/PS}$ are listed in *Table 2*. Examination of the electron micrographs of the binary blends containing 20 vol% B(130) or B(440) block copolymer shown in *Figures 2* and *3* indicates that both microphase and macrophase formation may occur. *Figure 4* shows that in the blends containing 80 vol% of B(440) and PVC(120), PVC(175) or PVC(275), long range fluctuations of the PVC concentration are observed, as evidenced by the appearance of PVC-rich regions and by the variation in the microstructural morphology between hexagonally packed cylinders and disordered spheres. Regions rich in

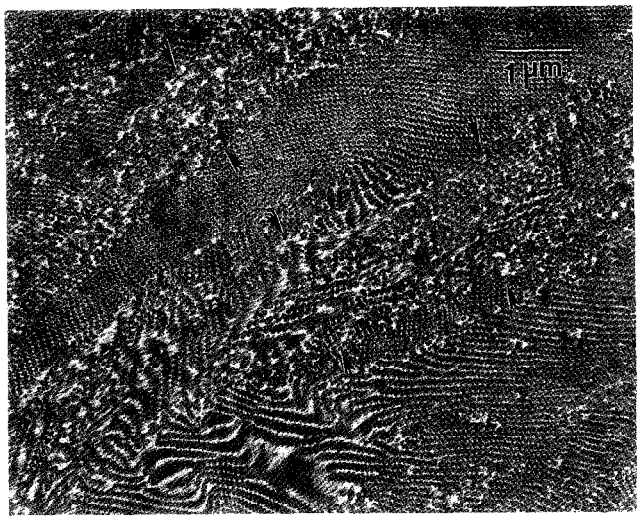

(a)

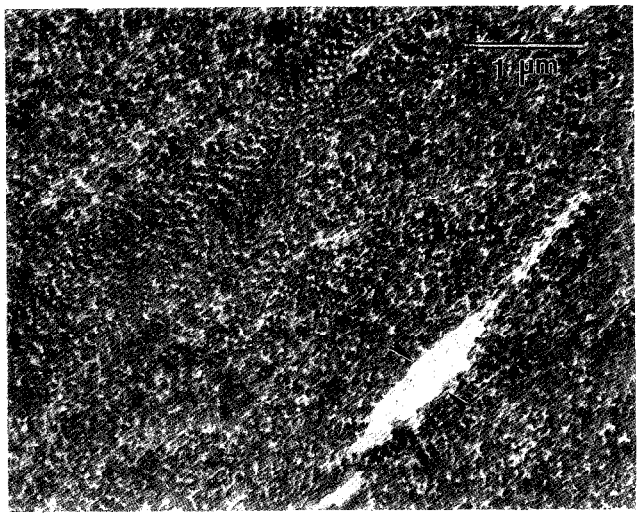

(b)

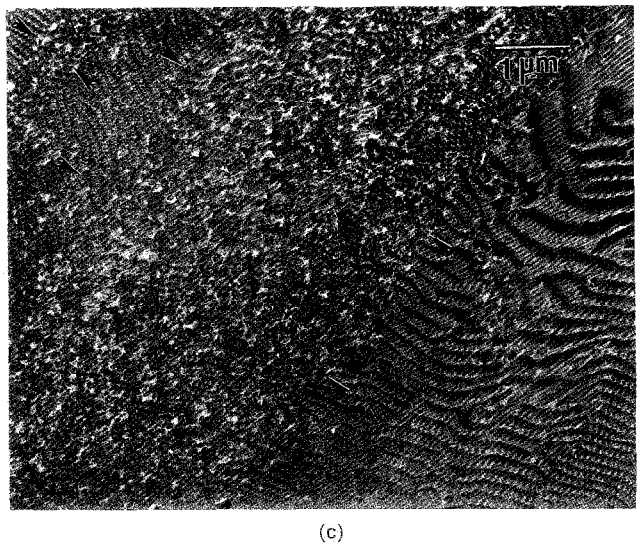

(c)

Figure 4 Variation in PVC concentration indicated by the fluctuation in the microstructure in blends containing 80 vol% B(440): (a) PVC(120)/B(440); (b) PVC(175)/B(440); (c) PVC(275)/B(440)

block copolymer contain the hexagonally packed cylinders and PVC-rich regions contain disordered spheres or almost pure PVC. These regions are delineated by arrows in *Figures 4a–c*. The microphase morphology in the 80 vol% B(440) blends can be explained to result from the creation of a region rich in block copolymer via macrophase separation, and hence can be described as macrophase-induced microphase[26].

From *Table 2*, it is clear that the M_h/M_x values in the PVC/B(130) blends are substantially greater than unity, which suggests that PVC should not be solubilized in the block copolymer and hence the macrophase should be formed[1,10]. However, microphase formation clearly occurs, as evidenced by the presence of the uniformly dispersed micelles shown in *Figures 2a–d*. This occurs because of the exothermic interaction of PVC with the PnBMA segment of the block copolymer[22–25,27–30]. However, in the PVC(500)/B(130) blend where a macrophase is also formed, as evidenced by the presence of PVC-rich regions in *Figure 2e*, micelles are present but weakly clustered. There are also a few PVC-rich regions in the PVC(78)/B(130) blends but they are very rare, and their origin is not yet understood since the product $N\chi_{PVC/PS}$ is minimal. The PVC-rich regions indicated by arrows in *Figure 2e* appear dark, not because they are stained but owing to thinning of the area covered by micelles on exposure to the illuminating electron beam. Thus they appear darker as the bright field images are obtained by mass/thickness contrast. The PVC-rich regions are bright at initial exposure but they become darker, even over the short period during which pictures are taken.

In contrast, for the PVC/B(440) blends, uniform microphase formation is observed only for PVC(78) (see *Figure 3a*). Clustered micellar macrophases are observed for the other PVC species (see *Figures 3b–e*). The macrophase morphology observed for PVC(120), PVC(175) and PVC(275) blends is an unexpected result since there is favourable exothermic mixing between the PVC and the PnBMA which leads one to expect only a microphase structure. Although the M_h/M_x ratio in the PVC(500)/B(440) blend is 2.22, the favourable exothermic mixing would be expected to aid microphase formation. It is worth mentioning that at higher magnification, the local micellar shape is ellipsoidal, i.e. the two principal surface curvatures are each positive[32]. The formation of elliptical micelles when $M_h/M_x > 1$ is an indication of strong swelling of the block copolymer segment by the homopolymer. In all blends where both a macrophase and microphase are formed, elliptical microdomains are formed which result from strong exothermic swelling of the PnBMA segment by PVC.

The tendency towards macrophase separation as measured by the incompatibility degree $N\chi_{PVC/PS}$, listed in *Table 2*, evidently increases on raising the molecular weight of either the PS block copolymer segment or PVC. By increasing the molecular weight of the PS block segment from 54 kDa to 215 kDa in the B(130) and B(440) block copolymers, respectively, or by systematically increasing the molecular weight of the PVC from 78 kDa to 120 kDa, 175 kDa, 275 kDa or 500 kDa, we have varied the magnitude of the incompatibility degree $N\chi_{PVC/PS}$ from 19 to 90. From *Figures 2* and *3*, there is a transition from uniformly dispersed microdomains to weakly clustered to strongly clustered

Table 2 Magnitude of the repulsion $N\chi_{PVC/PS}$ between PVC and the PS block segment, where the effective degree of polymerization is N[a]

		B(130)				B(440)			
	$10^{-3}M_w$	M_h/M_x	$N\chi_{PVC/PS}$	Microphase	Macrophase	M_h/M_x	$N\chi_{PVC/PS}$	Microphase	Macrophase
PVC(78)	78	1.03	19		×	0.35	39	×	
PVC(120)	120	1.58	22	×		0.53	49		×
PVC(175)	175	2.30	25	×		0.78	59		×
PVC(275)	275	3.62	29	×		1.22	72		×
PVC(500)	500	6.58	33		×	2.22	90		×

[a] $N = N_{PVC}N_{PS}/(N_{PVC}^{1/2} + N_{PS}^{1/2})^2$. The value $\chi_{PVC/PS} = 0.099\,16$ was obtained from the solubility parameter $\delta_{PVC} = 10.1$ and $\delta_{PS} = 9.33\,cal^{1/2}\,cm^{-3/2}$ and a molar volume of $99.0\,cm^3\,mol^{-1}$ at 25°C

microdomains as the magnitude of the incompatibility degree increases. Note that microphase separation is generated in blends containing B(440) when $N\chi_{PVC/PS}$ is reduced to 39 (M_w(PVC) = 78 kDa); the macrophase is induced in blends containing B(130) when $N\chi_{PVC/PS}$ is raised to 33. Unfortunately, we could not investigate the microstructures when $33 < N\chi_{PVC/PS} < 39$, since further decrease of the PVC molecular weight below 70 kDa makes the samples become unstable on exposure to the electron beam, and increasing the PVC molecular weight above 500 kDa increases the difficulty of dissolution in MEK. Also, we have available at present only two block copolymer molecular weights. The crossover from microphase to macrophase separation appears to occur when $N\chi_{PVC/PS} \approx 30$–$50$. Thus, the degree of incompatibility $N\chi_{PVC/PS}$ influences the final morphology, but the phase transition region for $N\chi_{PVC/PS} \approx 30$–$50$ is not universal.

In the second set of blends where 80 vol% of B(440) was used with three of the PVCs (120, 175 and 275), it was observed that macrophase separation still persisted, as evidenced by the presence of the PVC-rich regions indicated with arrows in *Figure 4b* and by the fluctuation in the shape of the microstructures (also indicated by arrows) in *Figures 4a* and *4b*. As mentioned above, hexagonally packed cylinders and disordered spherical microstructures are formed in different regions. The areas containing disordered spherical microdomains, which indicate regions rich in PVC, are marked off by arrows. The areas where hexagonally packed cylinders are formed are those of lower PVC concentration. The observation of such long range concentration fluctuations is a clear indication of macrophase separation followed by microphase separation. Clearly, if $M_{PVC} < M_{B,PnBMA}$ and the volume fraction of PVC is less than that of PnBMA, the macrophase separation cannot be attributed to coronal saturation. Instead, the driving force for macrophase separation is a large value of $N\chi_{PVC/PS}$. We note that the effect of the polydispersity of PVC on the phase-separated morphology should be considered. In principle, polydispersity can lead to fractionation of higher molecular weight chains into the PVC-rich macrophase regions and enhance the tendency for forming spherical micelles by accumulation of low molecular weight PVC chains in the phase rich in block copolymer. We expect such an effect to be small because of the exothermic nature of the PVC/PnBMA interaction. This is supported by the observation of the microphase in the blend containing B(130) and PVC(275) in which the molecular weight of PnBMA(74) is much less than that of PVC(275), and rejection of large PVC chains is expected to lead to macrophase separation.

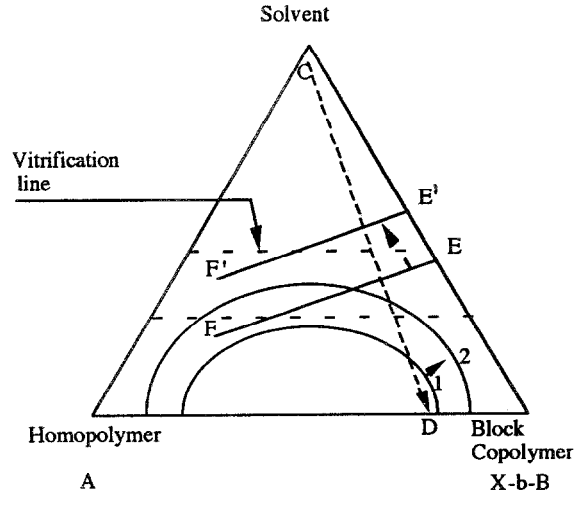

Figure 5 Equilateral triangular phase diagram showing the routes to the microphase and macrophase on changing the degree of repulsion between the homopolymer and the incompatible block copolymer segment

Finally, the competition between microphase and liquid/liquid macrophase separation can be interpreted via ternary phase diagrams. A similar approach was used by Hashimoto *et al.*[21] to describe microstructure transformation in solvent-cast mixtures of poly(phenylene oxide) (PPO) with poly(styrene-*b*-isoprene) (PS-*b*-PI). A typical representation of the routes of phase formation is presented in *Figure 5*. Generally, each vertex represents 100% of the labelled component. The line EF indicates the location of block copolymer microphase formation as solvent is removed. The line E′F′ shows that microphase separation will occur much earlier at higher block copolymer molecular weight. The boundary at which macrophase separation occurs is mapped out by curve 1. The immiscibility window increases, as indicated by an upward shift from curve 1 to curve 2, as the incompatibility between the homopolymer A and the incompatible segment B (i.e. $N\chi_{A/B}$) increases. The isopleth line CD traces the drying history of a very dilute blend of the homopolymer and block copolymer in the solvent from concentration C to solvent-free composition D. As the solvent is removed from the blend solution, the solvent concentration reaches a critical point where any structure that is

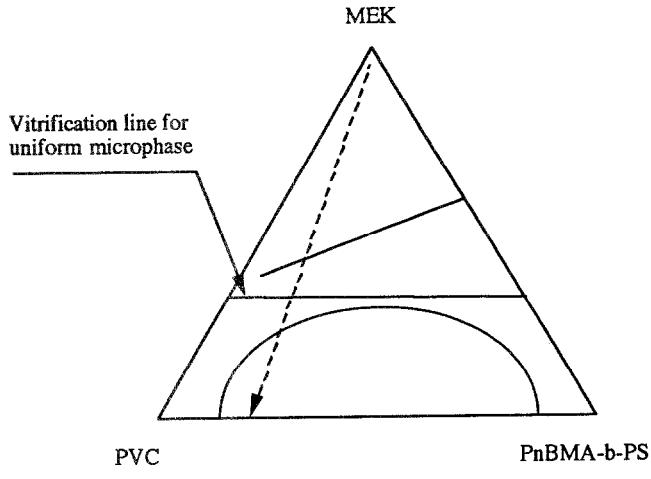

Figure 6 Schematic phase diagram of the microphase formation process in the blends showing weak repulsion

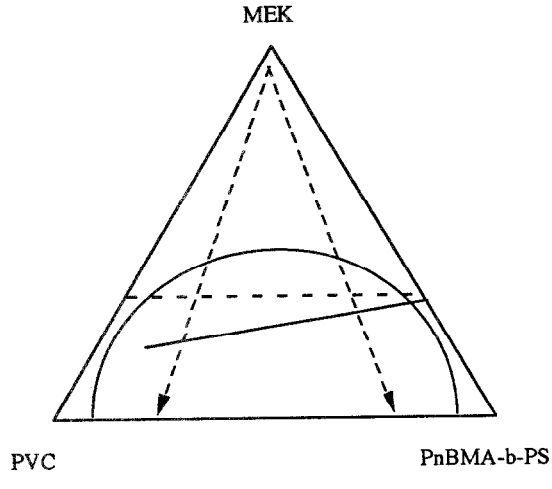

Figure 7 Schematic phase diagram of the macrophase separation process in the blends containing 20 or 80 vol% B(440) and showing strong repulsion

formed is frozen in as the mixture passes through its glass transition. These vitrification concentrations are indicated by the horizontal dotted lines. We recognize that the vitrification concentrations may not be accurately represented by the horizontal lines since the glass transition of the macrophase containing a higher concentration of the higher T_g block copolymer is expected to be at a higher solvent concentration than for the macrophase containing a higher concentration of lower T_g PVC. For example, if the macrophase is formed first and the vitrification concentration is reached before the onset of microphase separation, a non-equilibrium macrophase will be observed since the dissolution process will be hindered by the low mobility. Specifically, the schematic diagram shown in *Figure 5* explains the phase transition at low incompatibility degree (small $N\chi_{PVC/PS}$) in PVC/PnBMA-*b*-PS blends cast from MEK. When microphase separation occurs at E′F′, and macrophase at curve 1, this represents the route by which the uniform micellar microphases observed in *Figures 2b–d* and in *Figure 3a* are formed. This is more clearly explained in *Figure 6* in which the microphase is formed, followed by vitrification which inhibits the possibility of macrophase separation. In *Figure 5* we also show the case, symbolized by curve 2, when $N\chi_{PVC/PS}$ is sufficiently large that limited formation of a PVC-rich macrophase occurs (*Figure 2e*). In each of these cases, the incompatibility between the PVC and PS segments is weak as $N\chi_{PVC/PS}$ values range from 19 to 39. The formation of a PVC-rich macrophase further requires that the vitrification point lies just within the immiscibility window, i.e. curve 2. This is specifically illustrated in *Figure 7*, which represents the phase diagram for blends that underwent macrophase separation followed by micelle formation as shown in the electron micrographs in *Figures 3b–e* and *4a–c*. Diffusion of the micelle gas from the clustered arrangement to a uniform distribution is hindered by the vitrification point. In these blends, $N\chi_{PVC/PS}$ ranges from 49 to 90. Note that here the immiscibility window extends beyond the microphase line, and on descending the isopleth line the macrophase is formed, initially generating PVC-rich regions and regions rich in block copolymer. This process is followed by a secondary process of local rearrangement of the block copolymer chains to generate a microstructure. The microstructural geometries are mostly ellipsoidal and worm-like. Note that this process of secondary microstructure formation is different from the phenomenon of micellar clustering following formation of individual micelles as described by Lowenhaupt and Hellmann[6,7] and Lowenhaupt *et al.*[15].

In the blends containing 80 vol% B(440), the microstructure ranges from cylindrical micelles which are formed in the regions that are very deficient in PVC, to worm-like and spherical shapes as the concentration of PVC increases, and there are no micelles in the regions of almost pure PVC. Hence, the concentration fluctuation can be traced by the changes in the microstructural shape.

CONCLUSION

Morphological studies have been performed on binary blends containing a homopolymer and a block copolymer where there is exothermic mixing of the homopolymer with one of the block copolymer segments. The magnitude of the repulsion between the homopolymer and the incompatible block copolymer segment was changed by varying the molecular weight of each polymer. It has been clearly shown that the formation of a macrophase in these blends is not the result of low entropic swelling of the compatible segment since the microphase was formed at high M_h/M_x ratios in the blends containing B(130) and the macrophase was observed at low M_h/M_x ratios in the B(440) blends. Microphase and macrophase formation in such blends has thus been found to depend strongly on the thermodynamic product $N\chi_{PVC/PS}$, which characterizes the strength of the incompatibility between the homopolymer and the immiscible segment. The mechanism of the morphological transformation can be explained using triangular phase diagrams.

In addition, when a homopolymer is exothermically miscible with a segment of a block copolymer, it is clear that the homopolymer will strongly swell the compatible block copolymer segment even at M_h/M_x ratios greater than unity, where incompatibility is expected for isochemical blends. However, clustered microstructures derived from macrophase-induced microphase

separation may result when the repulsion between the homopolymer and the incompatible segment is very large. In such systems, therefore, it is not only possible to achieve microphase formation using a low molecular weight block copolymer, but in fact a low molecular weight block copolymer is necessary to produce the microphase when the molecular weight of the homopolymer is very large.

ACKNOWLEDGEMENT

We are pleased to acknowledge financial support from the National Science Foundation through Material Research Group award DMR 01845.

REFERENCES

1 Thomas, E. L. and Winey, K. I. *Proc. ACS Div. Polym. Mater. Sci. Eng.* 1990, **62,** 686
2 Winey, K. I., Thomas, E. L. and Fetters, L. J. *Macromolecules* 1991, **24,** 6182
3 Mayes, A. M. and Olvera de la Cruz, M. *Macromolecules* 1988, **21,** 2543
4 Kinning, D. J., Thomas, E. L. and Fetters, L. J. *J. Chem. Phys.* 1989, **90,** 5806
5 Kinning, D. J., Winey, K. I. and Thomas, E. L. *Macromolecules* 1988, **21,** 3502
6 Lowenhaupt, B. and Hellmann, G. P. *Polymer* 1991, **32,** 1065
7 Lowenhaupt, B. and Hellmann, G. P. *Colloid Polym. Sci.* 1990, **268,** 885
8 Tanaka, H., Hasegawa, H. and Hashimoto, T. *Macromolecules* 1991, **24,** 240
9 Koizumi, S., Hasegawa, H. and Hashimoto, T. *Makromol. Chem., Macromol. Symp.* 1992, **62,** 75
10 Jeon, K. J. and Roe, R. J. *Macromolecules* 1994, **27,** 2439
11 Tucker, P. S. and Paul, D. R. *Macromolecules* 1988, **21,** 2801
12 Braun, H., Rudolf, B. and Cantow, H. J. *Polym. Bull.* 1994, **32,** 241
13 Brown, H. R., Char, K. and Deline, V. R. *Macromolecules* 1990, **23,** 3383
14 Siqueira, D. F. and Nunes, S. P. *Polymer* 1994, **35,** 490
15 Lowenhaupt, B., Steurer, A., Hellmann, G. P. and Gallot, Y. *Macromolecules* 1994, **27,** 908
16 Tucker, P. S., Barlow, J. W. and Paul, D. R. *Macromolecules* 1988, **21,** 2794
17 Vilgis, T. A. and Noolandi, J. *Macromolecules* 1990, **23,** 2941
18 Akiyama, M. and Jamieson, A. M. *Polymer* 1992, **33,** 3582
19 Adedeji, A., Jamieson, A. M. and Hudson, S. D. *Macromolecules* 1994, **24,** 4018
20 Adedeji, A., Jamieson, A. M. and Hudson, S. D. unpublished results
21 Hashimoto, T., Kimishima, K. and Hasegawa, H. *Macromolecules* 1991, **24,** 5704
22 Leibler, L., Orland, H. and Wheeler, J. C. *J. Chem. Phys.* 1983, **79,** 3550
23 Adedeji, A., Jamieson, A. M. and Hudson, S. D. unpublished results
24 Cogan, K. A., Leermakers, F. A. M. and Gast, A. P. *Langmuir* 1992, **8,** 429
25 Hashimoto, T. *Phase. Trans.* 1988, **12,** 47
26 Koizumi, S., Hasegawa, H. and Hashimoto, T. *Macromolecules* 1994, **27,** 4371
27 Leibler, L. *Macromolecules* 1980, **13,** 1602
28 Walsh, D. J. and McKeown, J. G. *Polymer* 1980, **21,** 1335
29 Tremblay, C. and Prud'homme, R. E. *J. Polym. Sci., Polym. Phys. Edn* 1984, **22,** 1857
30 Kern, R. J. *J. Polym. Sci.* 1958, **33,** 524
31 Coleman, M. M. and Zarian, J. *J. Polym. Sci., Polym. Phys. Edn* 1979, **17,** 837
32 Hyde, S. T., Fogden, A. and Ninham, B. W. *Macromolecules* 1993, **26,** 6782